Surface Enrichment of Ag Atoms in Au/Ag Alloy Nanoparticles Revealed by Surface-Enhanced Raman Scattering of 2,6-Dimethylphenyl Isocyanide

Kwan Kim,*,† Kyung Lock Kim,† Jeong-Yong Choi,† Hyang Bong Lee,† and Kuan Soo Shin*,‡

Department of Chemistry, Seoul National University, Seoul 151-742, Korea, and Department of Chemistry, Soongsil University, Seoul 156-743, Korea

Received: November 26, 2009; Revised Manuscript Received: January 25, 2010

Surface-enhanced Raman scattering (SERS) of 2,6-dimethylphenyl isocyanide (2,6-DMPI) has been investigated with Au/Ag alloy nanoparticles as the adsorbing substrate. UV/visible spectra suggest the formation of alloy nanoparticles is taking place, in conformity with the mole fractions of gold and silver used initially in preparing the alloy sols; according to transmission electron microscopic images, the alloy sols are composed of spherical particles with diameters of ∼35 nm irrespective of their composition, from pure Ag to pure Au nanoparticles. We have confirmed that the SERS spectral feature of 2,6-DMPI on pure Ag is distinctly different from that on pure Au. Furthermore, the SERS spectral feature of 2,6-DMPI on Au/Ag alloy particles, even with a nominal composition of 95% Au and 5% Ag ($Au_{0.95}Ag_{0.05}$), is the same as that on pure Ag. The present observation supports our previous contention that the outermost layers of the Au/Ag alloy nanoparticles are highly enriched in Ag atoms compared with their interiors. SERS is thus proven to be an invaluable tool for the surface analysis of alloy metals.

1. Introduction

Over several decades, the properties of metal nanoparticles have been intensely investigated in conjunction with their potential use in microelectronics, chemical sensors, data storage, and a host of other applications.[1−5] This is related to the fact that metal nanoparticles have unique optical, electronic, and magnetic properties that are not found in either isolated atoms or bulk solids.[6−8] Due to their high surface-to-volume ratios, metal nanoparticles are also expected to function as effective catalysts.[9−14] Another noteworthy point is that the surface chemical properties of nanoparticles must be different from their bulk properties due to the inevitable presence of dangling bonds at the surface sites.[5] In alloy nanoparticles, the surface chemical composition may also be different from the interior part owing to intrinsically different surface tension characteristics of the constituent elements.[15−17] Such a compositional difference, though small, has to be considered seriously, especially for fabrication of nanoparticle-based microelectronic devices and sensors.

It is usually very difficult to analyze the outermost part of nanoparticles, even by using state-of-the-art analysis tools such as X-ray photoelectron spectroscopy and energy-dispersive X-ray spectroscopy. This is because the probing beams penetrate a finite distance into the bulk; the penetration depth of typical surface-analyzing methods such as X-ray fluorescence, electron-probe microanalysis, and particle-induced X-ray and γ-ray emission ranges at least from a few micrometers up to a few tens of micrometers.[18−20] As another example, Raman microscopy, and in particular confocal microscopy, is known to have very high spatial resolution, but the lateral and depth resolutions achievable are merely 250 nm and 1.7 μm, respectively, for a confocal Raman microspectrometer with the 632.8 nm line from a He−Ne laser with a pinhole of 100 μm diameter.[21] A more delicate surface-analyzing tool or an indirect method has thus to be devised to verify minute compositional differences between the surface and the interior bulk at the nanometer scale. A low-energy ion scattering method may be applied to the quantification of the outermost layer, but there is an inherent disadvantage in that the detectable signal becomes weak and irregular when the surface layer of a target substrate is gradually nanostructured; the method also requires a sophisticated ultrahigh vacuum system.[22] It is thus not surprising that, at micrometer scales, surface enrichment for gold or silver alloys has been reported by several authors, but reports on surface enrichment on nanometer scales are rare and scarcely found at all in the specific case of nanosized alloys.

Noble metallic nanostructures exhibit a phenomenon known as surface-enhanced Raman scattering (SERS) in which the scattering cross sections are dramatically enhanced for molecules adsorbed thereon; the most efficient metal is silver, followed by gold, copper, and transition metals.[23−25] In recent years, it has been reported that even single-molecule spectroscopy is possible by use of SERS, suggesting that the enhancement factor of Ag colloidal particles can reach as much as $10^{14}-10^{15}$; the Raman cross sections are then comparable to the usual fluorescence cross sections.[26] According to theoretical studies, at least 8−10 orders of magnitude must arise from electromagnetic surface plasmon excitation, while the enhancement factor due to chemical effect is presumed to be on the order of 10^1-10^2. In agreement with the electromagnetic and chemical enhancement mechanisms, SERS is especially sensitive to the first layer of substrates.

Au and Ag form homogeneous alloys when reduced by sodium citrate simultaneously. This is because Au and Ag have such similar lattice constants[27] that single-phase alloys can be achieved at any desired composition.[28,29] By referring to the fact that the SERS spectral feature of pyridine on Ag is slightly different from that on Au (which is associated with the surface selection rule of SERS), we have reported previously that, in

* To whom correspondence should be addressed. (K.K.) Tel +82-2-8806651; fax +82-2-8891568; e-mail kwankim@snu.ac.kr. (K.S.S.) Tel +82-2-8200436; fax +82-2-8244383; e-mail kshin@ssu.ac.kr..

† Seoul National University.

‡ Soongsil University.

10.1021/jp9112624
Published on Web 02/05/2010

Au/Ag alloy nanoparticles, Ag atoms are highly enriched at the outermost part of the nanoparticles compared with their interior part.[30] Although it was difficult to identify any difference in peak positions, there was a noticeable difference in relative peak intensities in the two cases. The selection rule of SERS is not yet established clearly, however, due to the complexity of the phenomenon. This is why more evidence is needed to support the previous contention that the outermost surfaces of Au/Ag alloy particles are highly enriched with Ag atoms. Apart from the peak intensity, vibrational frequency is the other important parameter of molecular structure. We found recently that organic isonitriles adsorb fairly well on metals including gold and silver, with their NC stretching frequencies being very susceptible to the kinds of metals adsorbed[31] as well as to the potentials applied to them.[32] In order to provide an additional clue to the surface enrichment, we have thus conducted a SERS study for 2,6-dimethylphenyl isocyanide (2,6-DMPI) adsorbed on Au/Ag alloy nanoparticle aggregates. In fact, we confirmed in this work that the surfaces of alloy nanoparticles with even a nominal composition of 95% Au and 5% Ag ($Au_{0.95}Ag_{0.05}$) are predominantly covered with Ag atoms, showing a SERS spectrum of 2,6-DMPI similar to that adsorbed on pure Ag nanoparticles.

2. Experimental Section

Silver nitrate ($AgNO_3$, 99+%), hydrogen chloroaurate ($HAuCl_4$, 99.99%), sodium citrate, and 2,6-DMPI were purchased from Aldrich and used as received. Other chemicals unless specified were of reagent grade, and highly pure water whose resistivity was greater than 18.0 MΩ·cm was used throughout.

The aqueous Au/Ag alloy sols, as well as pure Au sol, were prepared by following the recipes of Link et al.[28] To prepare Au sol, 95 mL of aqueous $HAuCl_4$ solution containing 5 mg of Au was brought to a boil, 5 mL of 1% sodium citrate was added therein under vigorous stirring, and boiling was continued for ~30 min. To prepare the Au/Ag alloy sols, only a predetermined number of moles of gold atoms was substituted with the equivalent number of moles of silver atoms in the form of silver nitrate, $AgNO_3$. The Ag sol was prepared by following the recipes of Lee and Meisel.[33] Initially, 45 mg of $AgNO_3$ was dissolved in 250 mL of water, and the solution was brought to a boil. A solution of 1% sodium citrate (5 mL) was then added to the $AgNO_3$ solution under vigorous stirring, and boiling was continued for ~30 min. According to the transmission electron microscopy (TEM) analyses, all the nanoparticles prepared in this work were spherical, and their average diameters were also comparable to one another at ~35 nm.

UV−visible (UV/vis) spectra were obtained with a SCINCO S-4100 spectrometer. TEM images were obtained with a JEM-200CX transmission electron microscope at 200 kV after placing a drop of the as-prepared sol onto Ni/Cu grids. Energy-dispersive X-ray (EDX) analyses were taken from a CM20 transmission electron microscope at 200 kV. Raman spectra were obtained by use of a Renishaw Raman system Model 2000 spectrometer equipped with an integral microscope (Olympus BH2-UMA). The 632.8 nm line from a 17 mW He/Ne laser (Spectra Physics Model 127) was used as the excitation source. Raman scattering was detected by use of 180° geometry with a Peltier cooled (−70 °C) charged-coupled device (CCD) camera (400 × 600 pixels). The laser beam was focused onto a spot approximately 2 μm in diameter with an objective microscope on the order of 20×. The data acquisition time was usually 90 s. The holographic grating (1800 grooves/mm) and the slit allowed the spectral resolution to be 1 cm^{-1}. The Raman band of a silicon wafer at 520 cm^{-1} was used to calibrate the spectrometer, and the accuracy of the spectral measurement was estimated to be better than 1 cm^{-1}.

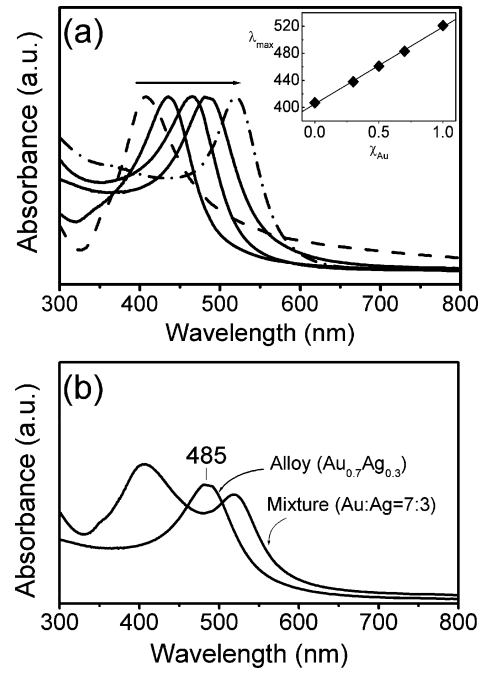

Figure 1. (a) UV/vis absorption spectra of Au/Ag alloy sols with varying gold mole fractions; the dashed and dash-dotted lines correspond to the pure Ag and Au nanoparticles, respectively. The spectra have been normalized at the plasmon absorption maxima. (Inset) Positions of maximum surface plasmon bands (λ_{max}) plotted against the mole fractions of Au (x_{Au}) in alloy nanoparticles. (b) UV/vis spectra of an $Au_{0.7}Ag_{0.3}$ alloy sol and a 7:3 mechanical mixture of Au and Ag sols.

In order to better interpret the SERS spectral features, we have separately performed a simple density functional theory (DFT) calculation. The binding energy of 2,6-DMPI with a single Au or Ag atom and the associated change in the frequency of the NC stretching vibration are computed with the Gaussian 03W suite at the B3LYP level theory.[34] LANL2DZ basis sets are used for the Au and Ag atoms, while 6-31G(d) basis sets are used for all atoms of 2,6-DMPI. The vibrational frequencies computed after the geometry optimization are scaled by 0.9659 for frequencies greater than 1800 cm^{-1} but by 0.9927 for those below 1800 cm^{-1} by consulting the literature.[35,36]

3. Results and Discussion

As reported by Link et al.,[28] Au/Ag alloy nanoparticles were formed when gold and silver ions were reduced simultaneously by sodium citrate in the same solution. This can be confirmed from the fact that only one plasmon band appears in the optical absorption spectra of the sols in the as-prepared state. Figure 1a shows the UV/vis absorption spectra of the Au/Ag alloy sols with varying gold content. The plasmon band is red-shifted, corresponding to an increasing amount of gold. In the inset in Figure 1a, the plasmon maximum (λ_{max}) is plotted against the gold mole fraction (x_{Au}) and a linear relationship is found. In Figure 1b, the UV/vis spectrum of a 7:3 mechanical mixture of the Au and Ag sols is shown, along with the spectrum taken for an alloy sol with a nominal composition of $Au_{0.7}Ag_{0.3}$, for reference. Two distinct surface plasmon bands are clearly in evidence in the spectrum of the mechanical mixture.

Metal colloids become aggregated upon addition of adsorbate molecules into the sol medium. The coagulation of sol particles

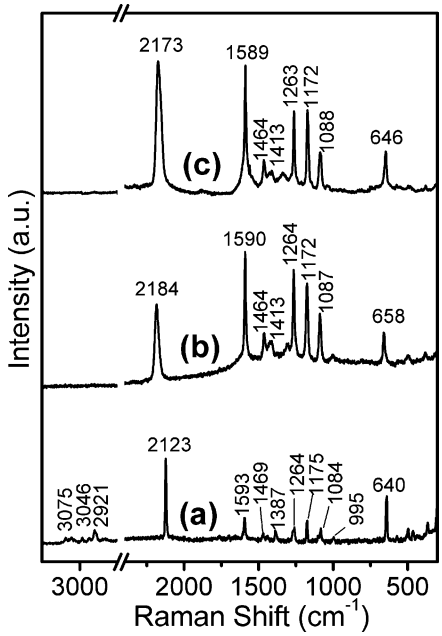

Figure 2. (a) Normal Raman spectrum of 2,6-DMPI in neat state. (b, c) SERS spectra of 2,6-DMPI adsorbed on (b) Au and (c) Ag nanoparticle films.

is also necessary for the particles to be SERS-active via an electromagnetic enhancement mechanism.[23,24] In fact, 2,6-DMPI induces a facile aggregation of Au and Ag colloids. The Au/Ag alloy sols also readily aggregate upon addition of 2,6-DMPI into the sols. The initial plasmon band gradually weakens, and a rather featureless band develops throughout the visible region, indicating the formation of stringlike aggregates[37] (data not shown). The SERS spectra of 2,6-DMPI can then be obtained by use of 632.8 nm radiation as the excitation source. We nonetheless took SERS spectra of 2,6-DMPI, not in the colloidal state but in the form of a film. We had already learned that the NC stretching frequency is very susceptible to the environment.[31,38] Although the wavelength of the surface plasmon resonance (SPR) band of Au/Ag alloy sols varies almost linearly with the bulk composition, the local environment of nanoparticles may not be the same in all sols.[37,39] The surface concentration of citrates, for instance, would differ from each other depending on the colloid, affecting the surface potential of metal nanoparticles and so resulting in different NC stretching frequencies.[32] Considering all this, the colloidal particles were first centrifuged and washed thoroughly with water to remove any surface chemicals including excess citrates. The cleaned Au/Ag nanoparticles were spread on a slide glass and 2,6-DMPI was subsequently allowed to adsorb onto it. The SERS spectra taken in this way had to have depended more on the surface composition of the Au/Ag alloy nanoparticles.

Figure 2b,c shows the SERS spectra of 2,6-DMPI adsorbed on Au and Ag nanoaggregates taken with 632.8 nm radiation as the excitation source. For reference, the normal Raman (NR) spectrum of 2,6-DMPI in its neat state is shown in Figure 2a. In the NR spectrum, two intense peaks are observed at 2123 and 640 cm^{-1} due to the NC stretching and C−NC stretching vibrations, respectively.[40] Ring-associated bands are comparatively less intense than the NC-associated bands, as can be evidenced from the peaks at 3046, 1593, and 995 cm^{-1} in Figure 2a that can be assigned to CH stretching, ring CC stretching (ν_{8a}), and in-plane ring breathing (ν_{12}) modes of 2,6-DMPI, respectively.[40] At first glance it appears that the spectral peaks in Figure 2b,c can be correlated with those in Figure 2a. However, a close examination reveals that substantial spectral differences exist, not only between the NR and SERS spectra of 2,6-DMPI but also between the two SERS spectra obtained from Ag and Au aggregates. When the SERS spectrum in Figure 2b is compared with the NR spectrum in Figure 2a, the most noticeable differences are associated with the NC stretching, ν_{8a} ring CC stretching, and C−NC stretching bands. The ν_{8a} band becomes very intense, while the C−NC band is slightly weakened upon adsorption on Au particles. In addition, the C−NC stretching peak is shifted by as much as 18 cm^{-1}, while the ν_{8a} peak is shifted by only 3 cm^{-1}. The more remarkable thing is that the NC stretching peak is shifted from 2123 to 2184 cm^{-1}. The NC stretching peak has thus blue-shifted by as much as 61 cm^{-1} upon adsorbing on Au. On the other hand, the NC stretching band has broadened considerably, from 5 to 20 cm^{-1}, whereas the ring-associated bands including ν_{8a} have broadened by at best 2 cm^{-1}. The substantial blue-shifting of the NC stretching mode can be understood as a function of the carbon lone-pair electrons in the isocyanide group having an antibonding character.[38,41] The donation of these electrons to gold should increase the strength of the NC bond. The substantial band broadening is associated with the vibrational energy relaxation channel provided by the direct contact of the NC group with the Au substrate. All of these spectral characteristics indicate that 2,6-DMPI must adsorb on Au exclusively by forming an Au−CN bond.

Similarly to the case of the adsorption of 2,6-DMPI on Au surface, the ν_{8a} band is strongly intensified when adsorbed on Ag nanoparticles. In addition, the peak positions as well as the band widths of the ring-associated modes are also comparable to those in the NR spectrum in Figure 2a. Noticeable spectral differences are found, however, in the NC group-related spectral regions. On the one hand, the C−NC band has blue-shifted by 6 cm^{-1} (appearing at 646 cm^{-1}) when adsorbed on Ag nanoparticles, in comparison with 18 cm^{-1} when adsorbed on Au nanoparticles. On the other hand, the NC stretching band is observed at 2173 cm^{-1} in Figure 2c; the latter frequency is ∼11 cm^{-1} smaller than that in Figure 2b. That is, the NC stretching band has blue-shifted by ∼50 cm^{-1} when adsorbed on Ag, compared to 61 cm^{-1} when adsorbed on Au. This would suggest that the antibonding electron-donating capability of 2,6-DMPI onto Ag is slightly weaker than that onto Au. It is understood that 2,6-DMPI must also adsorb on Ag by forming an Au−CN bond. The major peaks observed in the NR and SERS spectra of 2,6-DMPI on Au and Ag are collectively summarized in Table 1 along with their vibrational assignments.

The SERS spectra of 2,6-DMPI adsorbed on Au/Ag alloy surfaces composed of $Au_{0.3}Ag_{0.7}$, $Au_{0.5}Ag_{0.5}$, $Au_{0.7}Ag_{0.3}$, and $Au_{0.9}Ag_{0.1}$ nanoparticles are shown in Figure 3 panels a−d, respectively. The spectral patterns in Figure 3a−d all closely resemble that on Ag in Figure 2c. Not only the peak positions but also their bandwidths and relative intensities are invariant within the limits of experimental uncertainty. For instance, the relative peak intensities of the NC stretching and the ring 8a CC stretching bands are found to be 0.82 ± 0.1 in Figure 2c (i.e., in the SERS spectrum taken with pure Ag nanoparticles) and 0.83 ± 0.1 in Figure 3c (i.e., in the SERS spectrum taken with $Au_{0.7}Ag_{0.3}$ alloy nanoparticles), while the corresponding value is 0.60 ± 0.1 in Figure 2b (i.e., in the SERS spectrum taken with pure Au nanoparticles). These resemblances can be attributed to the exclusive enrichment of Ag atoms at the outermost layer of the alloy nanoparticles. One may argue that it could occur due to the comparatively larger SERS enhancement at the Ag atom sites than at the Au atom sites, but we

TABLE 1: Spectral Data and Vibrational Assignment of 2,6-DMPI[a]

	SERS (cm^{-1})		
NR	Au	Ag	assignment[b]
3075	3074	3074	2 (A_1)
1593	1590	1589	8a (A_1)
1469	1464	1464	19a (A_1)
1387	1413w	1413w	19b (B_2)
1264	1264	1263	3 (B_2)
1175	1172	1172	9b (B_2)
1084	1087	1088	13 (A_1)
995	1001w	999w	12 (A_1)
	Substituents		
2921		2922	$\nu_{as}(CH_2)$
2123	2184	2173	ν(NC)
1469	1464	1464	$\beta_s(CH_2)$
1264	1264	1263	$\gamma(CH_2)$
640	658	646	ν(C−NC)

[a] Abbreviation: w, weak [b] Based on refs 40 and 42−44.

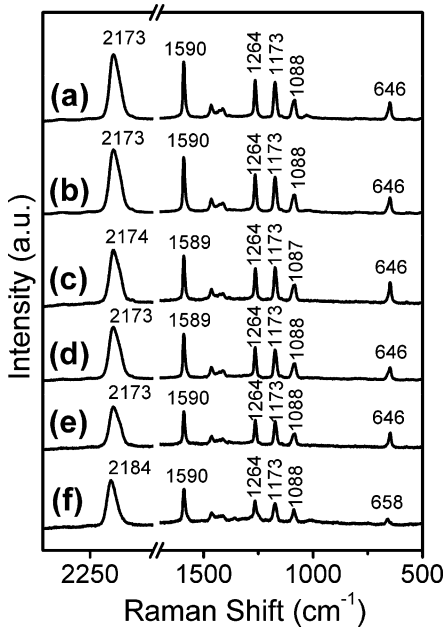

Figure 3. SERS spectra of 2,6-DMPI adsorbed on Au/Ag alloy films composed of (a) $Au_{0.3}Ag_{0.7}$, (b) $Au_{0.5}Ag_{0.5}$, (c) $Au_{0.7}Au_{0.3}$, (d) $Au_{0.9}Ag_{0.1}$, (e) $Au_{0.95}Ag_{0.05}$, and (f) $Au_{0.97}Ag_{0.03}$ alloy nanoparticles in bulk composition.

confirmed that the SERS enhancement factors on pure Au and Ag nanoaggregates are comparable to each other, at least for 632.8 nm excitation.

In principle, a 35-nm-sized Au/Ag core/shell nanoparticle with a single layer of Ag can be regarded to be composed of 95% Au and 5% Ag in a nominal composition. On this basis, we separately prepared two additional alloy sols with nominal compositions of $Au_{0.95}Ag_{0.05}$ and $Au_{0.97}Ag_{0.03}$. It is remarkable that the SPR band of $Au_{0.95}Ag_{0.05}$ appears at 517 nm, suggesting that its optical property is derived mainly from Au. As can be noticed from Figure 3e, the SERS spectral pattern of 2,6-DMPI suggests, however, that the outermost layer is still dominated by Ag atoms. In other words, the SERS spectral features are therefore the same for all alloys up to a nominal composition of $Au_{0.95}Ag_{0.05}$. As expected, the SERS spectrum taken with alloy particles with a nominal composition of $Au_{0.97}Ag_{0.03}$ in Figure 3f is obviously different from that taken with $Au_{0.95}Ag_{0.05}$ particles in Figure 3e. Rather, the SERS spectral pattern in

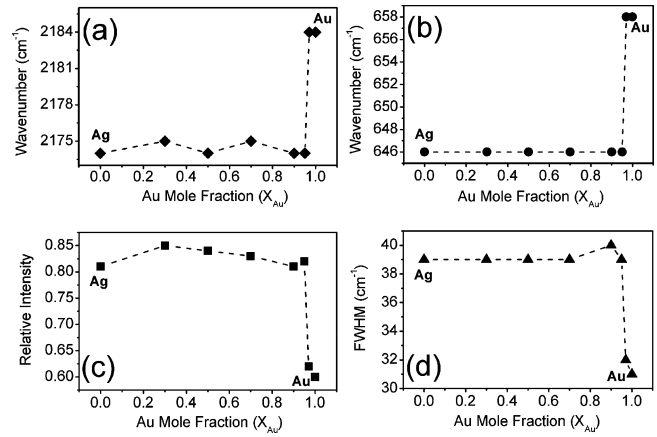

Figure 4. Peak positions of (a) NC and (b) C−NC stretching bands of 2,6-DMPI in Figure 3 plotted against the bulk composition of Au/Ag alloy nanoparticles. (c) Relative intensity of NC stretching and ring 8a CC stretching bands in Figure 3 drawn versus the bulk composition of Au/Ag alloy nanoparticles. (d) Full width at half-maximum (fwhm) of the NC stretching peak in Figure 3 against the mole fractions of Au (x_{Au}) in alloy nanoparticles.

Figure 3f resembles that of pure Au in Figure 2b. This is more clearly illustrated in Figure 4 where we show, on one hand, variation in the peak positions of the NC and C−NC stretching bands of 2,6-DMPI and, on the other hand, the relative intensities of NC and ring 8a CC stretching bands, as well as the bandwidth of the NC stretching peak, all drawn against the bulk composition of the Au/Ag alloy nanoparticles.

According to the EDX analyses, the Au:Ag ratios in $Au_{0.3}Ag_{0.7}$, $Au_{0.5}Ag_{0.5}$, and $Au_{0.7}Ag_{0.3}$ alloy particles are 28.8:71.2, 43.0:57.0, and 71.3:28.7, respectively. Considering the penetration depth in the EDX analysis, the data will not represent exactly the composition of the outermost layer or the overall nominal composition. Nevertheless, it is indeed intriguing that even the Au-rich alloy particles, that is, $Au_{0.7}Ag_{0.3}$, appear from SERS to be covered mostly with Ag atoms. At this point, it would be worth recalling the statement of Mulvaney[45] that, according to the Mie theory, one monolayer of gold should be sufficient to mask the silver plasmon band completely when Au was fully coated onto Ag nanoparticles. On the other hand, it will also be informative to recall that although the core−shell nanoparticles exhibit the same two absorption peaks, where one increases in absorbance with the increase in concentration of that component but with a concomitant decrease in absorbance of the other component,[46] only the SPR from the shell is detectable when the shell becomes thick enough.[47] If this prediction is correct, our Au/Ag alloy nanoparticles may not be covered fully with Ag atoms, since the surface plasmon maximum (λ_{max}) varies linearly against the gold mole fraction (x_{Au}), as shown in Figure 1b. One may also argue that when the rather broad absorbance near 400 nm in Figure 1a is considered, pure Ag nanoparticles may be copresent with alloy nanoparticles in the synthesized alloy sols. It has to be mentioned, however, that the surface plasmon band of Ag can be readily identified at ~400 nm, for instance, in the UV/vis spectrum of a 9:1 mechanical mixture of the Au and Ag sols, but the SERS spectrum of 2,6-DMPI adsorbed on the surface of a 9:1 mechanical mixture must be attributable entirely to that adsorbed on Au nanoparticles. It can be inferred, then, that the possibility of the presence of pure Ag nanoparticles in our synthesized alloy sols is extremely low.

If it is assumed that Au and Ag atoms are forming a close-packed face-centered cubic (fcc) structure with a comparable

TABLE 2: Binding Energies of 2,6-DMPI with Single Ag and Au Atoms and the Associated Changes in Bond Length and Stretching Frequency of the NC Group[a]

	2,6-DMPI	Ag−DMPI	Au−DMPI
binding energy, kJ/mol		−11.0	−53.6
NC bond length, nm	0.1182	0.1180	0.1179
NC stretching frequency,[b] cm^{-1}	2122	2163	2177

[a] Computed by use of the Gaussian 03W suite: LANL2DZ basis sets are used for Au and Ag atoms, while 6-31G(d) basis sets are used for all atoms of 2,6-DMPI. [b] Scaled by 0.9659 by referring to ref 36.

atomic radius of 0.144 nm, the number of metal atoms in a 35 nm nanoparticle is calculated to be 1.32×10^6. Among these metal atoms, the number of atoms residing at the outermost layer is estimated to be 5.4×10^4; the number of atoms remaining inside the nanoparticle will then be 1.27×10^6. If it is assumed that the outermost layer of an $Au_{0.7}Ag_{0.3}$ alloy nanoparticle is composed entirely of Ag atoms, the number of Ag atoms existing inside the nanoparticle must be 3.42×10^5. The ratio of Au and Ag atoms inside the nanoparticle may then be 0.73:0.27. It is noteworthy that this ratio is still not very different from the actual nominal ratio of the alloy nanoparticles, 0.7:0.3. The surface plasmon frequency of a hypothetical $Au_{0.73}Ag_{0.27}$ alloy sol is predicted to be 497 nm, if it is assumed that the surface plasmon frequency varies linearly as a function of Au content. If such nanoparticles become sparsely covered with Ag atoms, the surface plasmon frequency will be slightly blue-shifted, as is actually observed for an $Au_{0.7}Ag_{0.3}$ alloy sol at 485 nm, as shown in Figure 1a.

According to the temperature-dependent SERS study,[35] the binding energy of phenyl isocyanide on silver is lower than that on gold. For instance, *p*-biphenyl isocyanide was found by Kim et al.[35] to desorb from Ag at ~393 K, whereas the molecule remained stable up to ~453 K on Au. A DFT calculation has led to the same conclusion. As described in the Experimental Section, we also conducted a simple quantum mechanical DFT calculation by considering only a single Au (or Ag) atom interacting with a 2,6-DMPI molecule. As collectively summarized in Table 2, the binding energy is computed to be −53.6 kJ/mol for the Au−DMPI system but −11.0 kJ/mol for the Ag−DMPI system. It suggests that in equal conditions the phenyl isocyanide must adsorb on Au more favorably than on Ag. On the other hand, the NC stretching frequencies are computed to be 2122 cm^{-1} for free 2,6-DMPI but 2163 and 2177 cm^{-1} for the Ag−DMPI and Au−DMPI systems, respectively. That is, the NC stretching peak is computed to blue-shift by 41 and 55 cm^{-1} upon binding to Ag and Au atoms, respectively. These peak shifts, at least qualitatively, agree well with the experimental data shown in Figure 2. We previously argued that the blue shift of the NC stretching vibration is associated with the donation of the antibonding electrons of the isocyanide group to Au or Ag. In agreement with the explanation, the bond length of the NC group in 2,6-DMPI is computed to decrease from 0.1182 nm to 0.1180 and 0.1179 nm, respectively, upon binding to Ag and Au atoms. Even if all these computed results are taken into consideration, the observation that the SERS spectrum of 2,6-DMPI on $Au_{0.95}Ag_{0.05}$ particles is the same as that on pure Ag leads us to the conclusion that the Ag atoms must be enriched in the outermost layers of the Au/Ag alloy nanoparticles compared with their interiors.

4. Summary and Conclusion

Spherical Au/Ag alloy particles with a mean diameter of ~35 nm were successfully fabricated. The surface plasmon resonance of alloy particles varied from 400 to 520 nm in proportion to the molar content of Au in Au_xAg_{1-x}. After a thorough washing with water and ethanol, these alloy particles were dropped onto glass slides to act as as SERS substrates for 2,6-DMPI. Very distinct SERS spectra were obtained from all Au/Ag alloy films with 632.8 nm radiation as the excitation source. The peak positions as well as the bandwidths of the benzene ring modes were, in all SERS spectra, only slightly different from those in the normal Raman spectrum of neat 2,6-DMPI. The NC group-related bands were, however, significantly affected by the adsorption onto Au/Ag alloy particles. For instance, the NC stretching bands were seen to have blue-shifted, compared to the NR peak position, by up to 61 and 50 cm^{-1}, respectively, when adsorbed on pure Au and Ag nanoparticle films. The blue shift can be understood by considering the donation of the lone-pair electrons of the isocyanide group of 2,6-DMPI, having an antibonding character, to Au and/or Ag. An exciting observation was that not only the peak positions and the bandwidths, including those of the NC stretching vibration, but also the relative peak intensities were barely different from one another in all SERS spectra of 2,6-DMPI as long as the molar content of Ag was greater than 5% in Au/Ag alloy nanoparticles. That is, even the SERS spectrum of 2,6-DMPI on $Au_{0.95}Ag_{0.05}$ particles is nearly the same as that on pure Ag. The present observation supports our previous contention that the Ag atoms are highly enriched in the outermost layers of the Au/Ag alloy nanoparticles compared with their interiors, proving also that SERS is an invaluable tool for the surface analysis of alloy metals.

Acknowledgment. This work was supported by the Korea Science and Engineering Foundation (Grants R11-2007-012-02002-0 and M10703001067-08M0300-06711-Nano2007-02943) and the Korea Research Foundation (Grants KRF-2008-313-C00390 and 2009-0072467).

References and Notes

(1) Kreibig, U.; Vollmer, M. *Optical Properties of Metal Clusters*; Springer: Berlin, 1995.
(2) Kelly, K. L.; Coronado, E.; Zhao, L. L.; Schatz, G. C. *J. Phys. Chem. B* **2003**, *107*, 668.
(3) Link, S.; El-Sayed, M. A. *Annu. Rev. Phys. Chem.* **2003**, *54*, 331.
(4) Liz-Marzán, L. M. *Langmuir* **2006**, *22*, 32.
(5) Henglein, A. *Chem. Rev.* **1989**, *89*, 1861.
(6) Krenn, J. R.; Dereux, A.; Weeber, J. C.; Bourrillot, E.; Lacoute, Y.; Coudonnet, J. P. *Phys. Rev. Lett.* **1999**, *82*, 2590.
(7) Wang, L.; Shi, X.; Kariuki, N. N.; Schadt, M.; Wang, G. R.; Rendeng, Q.; Choi, J.; Luo, J.; Lu, S; Zhong, C.-J. *J. Am. Chem. Soc.* **2007**, *129*, 2161.
(8) Berkowitz, A. E.; Rodriguez, G. F.; Hong, J. I.; An, K.; Hyeon, T.; Agarwal, N.; Smith, D. J.; Fullerton, E. E. *Phys. Rev. B* **2008**, *77*, 024403.
(9) Yonezawa, T.; Toshima, N. *J. Mol. Catal.* **1993**, *83*, 167.
(10) Yen, C.-W.; Lin, M.-L.; Wang, A.; Chen, S.-A.; Chen, J.-M.; Mou, C.-Y. *J. Phys. Chem. C* **2009**, *113*, 17831.
(11) Comotti, M.; Li, W. C.; Spliethoff, B.; Schüth, F. *J. Am. Chem. Soc.* **2006**, *128*, 917.
(12) Demirok, U. K.; Laocharoensuk, R.; Manesh, K. M.; Wang, J. *Angew. Chem., Int. Ed.* **2008**, *47*, 9349.
(13) Wang, L.; Shi, X.; Kariuki, N. N.; Schadt, M.; Wang, G. R.; Rendeng, Q.; Choi, J.; Luo, J.; Lu, S.; Zhong, C. J. *J. Am. Chem. Soc.* **2007**, *129*, 2161.
(14) Wang, C.; Yin, H.; Chan, R.; Peng, S.; Dai, S.; Sun, S. *Chem. Mater.* **2009**, *21*, 433.
(15) Sun, Y.; Wiley, B.; Li, Z.-Y.; Xia, Y. *J. Am. Chem. Soc.* **2004**, *126*, 9399.
(16) Lu, X.; Au, L.; McLellan, J.; Li, Z.-Y.; Marquez, M.; Xia, Y. *Nano Lett.* **2007**, *7*, 1764.

(17) Zhu, J. *J. Phys. Chem. C* **2009**, *113*, 3164.
(18) Osán, J.; Szalóki, I.; Ro, C.-U.; Van Grieken, R. *Microchim. Acta* **2000**, *132*, 349.
(19) Cesareo, R.; Gigante, G. E.; Castellano, A.; Rosales, M. A.; Aliphat, M.; de la Fuente, F.; Meitin, J. J.; Mendoza, A.; Iwanczyk, J. B.; Pantazis, J. *J. Trace Microprobe Techn.* **1996**, *14*, 711.
(20) Guerra, M. F. *X-Ray Spectrom.* **1998**, *27*, 731.
(21) Renoupez, A. J.; Lebas, K.; Bergeret, G.; Rousset, J. L.; Delichère, P. *Stud. Surf. Sci. Catal.* **1996**, *101*, 1105.
(22) Allakhverdiev, K. R.; Lovera, D.; Altstadt, V.; Schreier, P.; Kador, L. *Rev. Adv. Mater. Sci.* **2009**, *20*, 77.
(23) Chang, R. K.; Furtak, T. E. *Surface Enhanced Raman Scattering*; Plenum Press, New York, 1982.
(24) Moskovits, M. *Rev. Mod. Phys.* **1985**, *7*, 209.
(25) Tian, Z. Q.; Ren, B.; Wu, D. T. *J. Phys. Chem. B* **2002**, *106*, 9463.
(26) Kneipp, K.; Kneipp, H.; Itzkan, I.; Dasari, R. R.; Feld, M. S. *Chem. Rev.* **1999**, *99*, 2957.
(27) Okamoto, H.; Massalski, T. B. In *Phase Diagrams of Binary Gold Alloys*; ASM International: Materials Park, OH, 1987.
(28) Link, S.; Wang, Z. L.; El-Sayed, M. A. *J. Phys. Chem. B* **1999**, *103*, 3529.
(29) Mallin, M. P.; Murphy, C. J. *Nano Lett.* **2002**, *2*, 1235.
(30) Kim, K.; Kim, K. L.; Lee, S. J. *Chem. Phys. Lett.* **2005**, *403*, 77.
(31) Kim, N. H.; Kim, K. *J. Phys. Chem. B* **2006**, *110*, 1873.
(32) Shin, D.; Kim, K.; Shin, K. S. *ChemPhysChem* **2010**, *11*, 83.
(33) Lee, P. C.; Meisel, D. *J. Phys. Chem.* **1982**, *86*, 3391.
(34) Frisch, M. J.; Trucks, G. W.; Schlegel, H. B.; Scuseria, G. E.; Robb, M. A.; Cheeseman, J. R.; Montgomery, J. A., Jr.; Vreven, T.; Kudin, K. N.; Burant, J. C.; Millam, J. M.; Iyengar, S. S.; Tomasi, J.; Barone, V.; Mennucci, B.; Cossi, M.; Scalmani, G.; Rega, N.; Petersson, G. A.; Nakatsuji, H.; Hada, M.; Ehara, M.; Toyota, K.; Fukuda, R.; Hasegawa, J.; Ishida, M.; Nakajima, T.; Honda, Y.; Kitao, O.; Nakai, H.; Klene, M.; Li, X.; Knox, J. E.; Hratchian, H. P.; Cross, J. B.; Bakken, V.; Adamo, C.; Jaramillo, J.; Gomperts, R.; Stratmann, R. E.; Yazyev, O.; Austin, A. J.; Cammi, R.; Pomelli, C.; Ochterski, J. W.; Ayala, P. Y.; Morokuma, K.; Voth, G. A.; Salvador, P.; Dannenberg, J. J.; Zakrzewski, V. G.; Dapprich, S.; Daniels, A. D.; Strain, M. C.; Farkas, O.; Malick, D. K.; Rabuck, A. D.; Raghavachari, K.; Foresman, J. B.; Ortiz, J. V.; Cui, Q.; Baboul, A. G.; Clifford, S.; Cioslowski, J.; Stefanov, B. B.; Liu, G.; Liashenko, A.; Piskorz, P.; Komaromi, I.; Martin, R. L.; Fox, D. J.; Keith, T.; Al-Laham, M. A.; Peng, C. Y.; Nanayakkara, A.; Challacombe, M.; Gill, P. M. W.; Johnson, B.; Chen, W.; Wong, M. W.; Gonzalez, C.; Pople, J. A. Gaussian 03W, revision C.01; Gaussian, Inc.: Wallingford CT, 2004.
(35) Kim, S.; Ihm, K.; Kang, T.-H.; Hwang, S.; Joo, S.-W. *Surf. Interface Anal.* **2005**, *37*, 294.
(36) Gruenbaum, S. M.; Henney, M. H.; Kumar, S.; Zou, S. *J. Phys. Chem. B* **2006**, *110*, 4782.
(37) Blatchford, C. G.; Campbell, J. R.; Creighton, J. A. *Surf. Sci.* **1982**, *120*, 435.
(38) Kim, H. S.; Lee, S. J.; Kim, N. H.; Yoon, J. K.; Park, H. K.; Kim, K. *Langmuir* **2003**, *19*, 6701.
(39) Creighton, J. A.; Blatchford, C. G.; Albrecht, M. G. *J. Chem. Soc., Faraday Trans. 2* **1979**, *75*, 790.
(40) Joo, S.-W.; Kim, W.-J.; Yun, W. S.; Hwang, S.; Choi, I. S. *Appl. Spectrosc.* **2004**, *58*, 218.
(41) Ontko, A. C.; Angelici, R. J. *Langmuir* **1998**, *14*, 1684.
(42) Varsany, G. *Assignments for Vibrational Spectra of Seven Hundred Benzene Derivatives*; Wiley: New York, 1974.
(43) Bae, S. J.; Lee, C. L.; Choi, I. S.; Hwang, C. S.; Gong, M. S.; Kim, K.; Joo, S.-W. *J. Phys. Chem. B* **2002**, *106*, 7076.
(44) Ikeda, K.; Fujimoto, N.; Uehara, H.; Uosaki, K. *Chem. Phys. Lett.* **2008**, *460*, 205.
(45) Mulvaney, P. *Langmuir* **1996**, *12*, 788.
(46) Mallik, K.; Mandal, M.; Pradhan, N.; Pal, T. *Nano Lett.* **2001**, *1*, 319.
(47) Lu, L.; Wang, H.; Zhou, Y.; Xi, S.; Zhang, H.; Hu, J.; Zhao, B. *Chem. Commun.* **2002**, 144.

JP9112624